

# UHPLC-Orbitrap screening of oleraindoles in hydromethanolic extracts of *Portulaca oleracea*

Yulian Voynikov<sup>1</sup>, Reneta Gevrenova<sup>1</sup>, Dimitrina Zheleva-Dimitrova<sup>1</sup>, Vessela Balabanova<sup>1</sup>, Irina Nikolova<sup>1</sup>, Lyubomir Marinov<sup>1</sup>, Iossif Benbassat<sup>1</sup>, Georgi Momekov<sup>1</sup>

<sup>1</sup> Faculty of Pharmacy, Medical University of Sofia, 2 Dunav str., 1000 Sofia, Bulgaria

Corresponding author: Yulian Voynikov (y\_voynikov@pharmfac.mu-sofia.bg)

Received 2 October 2023 ♦ Accepted 1 November 2023 ♦ Published 18 December 2023

**Citation:** Voynikov Y, Gevrenova R, Zheleva-Dimitrova D, Balabanova V, Nikolova I, Marinov L, Benbassat I, Momekov G (2023) UHPLC-Orbitrap screening of oleraindoles in hydromethanolic extracts of *Portulaca oleracea*. Pharmacia 70(4): 1521–1527. <https://doi.org/10.3897/pharmacia.70.e113577>

## Abstract

Purslane (*Portulaca oleracea* L., Portulacaceae) is a widespread edible plant with significant ethnobotanical and ethnopharmacological importance. The plant is characteristic for the presence of a class of indoline amide glucoside alkaloids, called cyclo-dopa amides, or oleraceins. Additionally, a new, structurally similar to oleraceins, class of indole amides have been discovered recently, called oleraindoles. These compounds have been evaluated to possess antiinflammatory and anticholinesterase activities. Herein, utilizing UHPLC-Orbitrap-MS with MS<sup>2</sup> filtering by diagnostic ion filtering (DIF), and diagnostic difference filtering (DDF) using different data analysis tools, eight compounds with oleraindole structure were tentatively identified.

## Keywords

Oleraindole, *Portulaca oleracea*, UHPLC, Orbitrap

## Introduction

The most popular analytical technique for high throughput plant metabolomics analysis is ultra-high-performance liquid chromatography coupled with high-resolution mass spectrometry (UHPLC-HRMS). Ions are resolved typically within 5 ppm error that allows the chemical composition of ions to be determined with high accuracy and precision, which is crucial in metabolite annotation. In addition, a variety of electronic spectral databases and MS data analysis software packages have been developed to aid in the structural elucidation of unknowns (Perez de Souza et al. 2017). However, many MS<sup>2</sup> spectral libraries still cover a small portion of the metabolome and are often not freely available (Stein 2012). As an alternative, MS<sup>2</sup> data filtering can be applied based on specific spectral features for a certain class of compounds, as neutral loss-,

diagnostic fragment ions-, and *m/z* differences filtering. One of the most popular platforms for LC-MS data processing, analysis, and visualization, is MZmine (Pluskal et al. 2010). One feature of this software package is the filtering of MS<sup>2</sup> spectra by diagnostic ions. A neutral loss filter is as well available; however, it applies to the specific *m/z* difference between the precursor ion and each of its fragment ions. Another software, called MS<sup>2</sup> analyzer (Ma et al. 2014), in addition to diagnostic ion- and neutral loss filtering, offers a *m/z* differences filtering. This feature performs *m/z* differences search between every fragment (including the precursor ion, even if it is not present in the MS<sup>2</sup> spectrum) and all lower *m/z* fragment ions.

Purslane (*Portulaca oleracea* L., Portulacaceae) is a widely distributed annual plant growing in many parts of the world. Purslane is consumed in soups and salads in many areas of Europe, the Mediterranean, and tropical

Asian countries (Petropoulos et al. 2019; Melilli et al. 2020; Corrado et al. 2021) and used in folk and traditional medicine (Akbar 2020). Various bio-active compounds have been isolated from purslane extracts, as flavonoids, polysaccharides, fatty acids, vitamins and minerals, and alkaloids (Akbar 2020; Kumar et al. 2021). Among alkaloids, purslane is characteristic for the presence of the so called cyclo-dopa amides, or oleraceins (Xiang et al. 2005; Xing et al. 2008; Jiao et al. 2014; Jiao et al. 2015; Voynikov et al. 2019; Fu et al. 2021). These are indoline amide glycosides that possess 5,6-dihydroxyindoline-2-carboxylic acid *N*-acylated with cinnamic acid derivatives, as a common scaffold. So far, more than 30 representatives of this class of natural compounds have been isolated (Xiang et al. 2005; Jiao et al. 2015; Fu et al. 2021), and even more have been tentatively identified (Xing et al. 2008; Jiao et al. 2014; Farag and Shakour 2019; Voynikov et al. 2019, 2021b). Just recently, by utilizing UHPLC-Orbitrap-MS we tentatively identified 51 representatives of this class of natural compounds (Voynikov et al. 2021b).

Recently, a new class of indole amides, called oleraindoles, have been isolated from purslane extracts (Zhao et al. 2019; Xu et al. 2020a, b). These compounds are structurally similar to oleraceins; instead of a *N*-acylated 5,6-dihydroxyindoline-2-carboxylic acid (the characteristic scaffold for oleraceins), oleraindoles are characterized with 5,6-dihydroxyindole, as the common scaffold (Fig. 2). Zhao et al. (Zhao et al. 2019) were the first to isolate oleraindole A (*N*-coumaroyl 5,6-dihydroxyindole) and oleraindole B (*N*-feruloyl 5,6-dihydroxyindole). A year later, Xu et al. (Xu et al. 2020a) isolated oleraindole C (*N*-caffeoyl 5,6-dihydroxyindole) and recently, a 6-glucoconjugate of oleraindole A was isolated from Xu et al. (Xu et al. 2020b), named oleraindole D (*N*-coumaroyl-6-O-glucosyl-5,6-dihydroxyindole). All four oleraindole representatives have been isolated from hydroethanolic extracts of purslane. Later, Lan et al. (Lan et al. 2022a) isolated and characterized a new oleraindole molecule, namely (E)-3-(4-hydroxy-3-methoxyphenyl)-1-(5-hydroxy-6-((3,4,5-trihydroxy-6-(hydroxymethyl)tetrahydro-2H-pyran-2-yl)oxy)-1H-indol-1-yl)prop-2-en-1-one, abbreviated as  $\beta$ -D-Glc-Oleraindole G. By the abbreviation used in our previous article (Voynikov et al. 2021a; for details refer to the section Used abbreviations in Materials and Methods) the structure of the compound is essentially **GGIC**. **GGIC** displayed anti-inflammatory activity at 20  $\mu$ M (Lan et al. 2022a). The same group of Lan et al. (Lan et al. 2022b) isolated and characterized two new oleraindoles, namely (E)-3-(4-hydroxy-3-methoxyphenyl)-1-(5-hydroxy-6-((3,4,5-trihydroxy-6-(hydroxymethyl)tetrahydro-2H-pyran-2-yl)oxy)-1H-indol-1-yl)prop-2-en-1-one and (E)-3-(4-hydroxy-3-methoxyphenyl)-1-(5-hydroxy-6-((3,4,5-trihydroxy-6-(hydroxymethyl)tetrahydro-2H-pyran-2-yl)oxy)-1H-indol-1-yl)prop-2-en-1-one, which have the structure of **GIF** and **GIC**, respectively. Both **GIT** and **GIC** demonstrated anti-inflammatory activities on RAW264.7 cells at 20  $\mu$ M (Lan et al. 2022b). Oleraindole A and B both demonstrated greater radical scavenging activity against the DPPH radical compared to the standard

butylated hydroxyanisole (Zhao et al. 2019). Also, Oleraindoles A, B, and D demonstrated comparable anticholinesterase activity to the standard eserine (Zhao et al. 2019; Xu et al. 2020a).

And thus, by utilizing UHPLC-Orbitrap-MS, we sought to screen more oleraindole structures in hydromethanolic extracts of purslane. The raw MS<sup>2</sup> data was filtered by diagnostic ion filtering (DIF) and diagnostic difference filtering (DDF) to select compounds bearing oleraindole structure, using the R programming language.

## Materials and methods

### Plant material

*Portulaca oleracea*, L. aerial parts were gathered from v. Orizovo, Bulgaria (42.208889°N, 25.170278°E) and identified by one of us (V.B.). Voucher specimens were deposited at the Faculty of Pharmacy, Medical University, Sofia, Bulgaria (Herbarium Facultatis Pharmaceuticae Sophiensis № 1563-1574).

### Extraction and sample preparation

Air-dried aerial parts of purslane were powdered, 3.00 g of plant material were extracted twice by sonication with 10 ml 70% MeOH at 50 °C for 15 min in an ultrasonic bath. The combined extracts were filtered and diluted with 70% MeOH to 25 ml in volumetric flasks. The extracts were diluted 10-fold before injection into the UHPLC-MS system, to a concentration of approx. 0.1 mg/ml.

### UHPLC-HR-MS instrument

The UHPLC system consisted of Dionex UltiMate 3000 RSLC HPLC, equipped with SRD-3600 solvent rack degasser, HPG-3400RS binary pump with solvent selection valve, WPS-3000TRS thermostated autosampler, and TCC-3000RS thermostated column compartment (Thermo Fisher Scientific). The UHPLC system was controlled by Chromeleon 7.2. The effluents were connected on-line with a Q Exactive Plus Orbitrap mass spectrometer (Thermo Fisher Scientific) equipped with a heated electrospray ionization (HESI-II) probe.

### Chromatographic parameters

Elution was carried out on a Kromasil EternityXT C18 (1.8  $\mu$ m, 2.1  $\times$  100 mm) column maintained at 40 °C. The binary mobile phase consisted of 0.1% formic acid in water (A), and 0.1% formic acid in acetonitrile (B). The chromatographic elution was as follows: the mobile phase was held at 5% B for 0.5 min and then gradually turned to 33% B over 19.5 min. Next, % B was increased gradually to 95% over 1 min and maintained at 95% B for 2 min. The system was turned to the initial condition of 5% B in 1 min and re-equilibrated over 4 min. The flow rate and the injection volume were set to 300  $\mu$ L/min and 1  $\mu$ L, respectively.

## Mass spectrometric parameters

A stepped 20–70 NCE was selected for initial screening of oleraindoles. Mass spectrometric parameters for Full-scan MS were as follows: resolution 17,500; AGC target 1e6; Maximum IT 83 ms; Scan range 290–1000  $m/z$ . For dd-MS<sup>2</sup>, the following parameters were used: TopN 10; isolation window 1.0  $m/z$ ; stepped NCE 20–70; Minimum AGC target 8.00e3; Intensity threshold 9.6e4; Apex trigger 2 to 6 sec; Dynamic exclusion 3 sec. The structural elucidation of the oleraindoles was achieved by manual inspection of the MS<sup>2</sup> spectra in Xcalibur 4.2 software (Thermo Fisher Scientific).

## Mass spectral filtering by Diagnostic Ion Filtering (DIF) and Diagnostic Difference Filtering (DDF)

Vendor \*.raw (Thermo Fisher Scientific) files were converted to either \*.mzML files or \*.mgf files by MSConvertGUI 3.0 (ProteoWizard) (French et al. 2015). MZmine 2.53 (Pluskal et al. 2010), MS<sup>2</sup>Analyzer (Ma et al. 2014) and an in-house script in the R programming language (4.3.1), using RStudio (“Mountain Hydrangea” Release (547dcf86, 2023-07-07) for windows; Posit Software, PBC) were used for DIF and DDF. Details on the script can be found in the Suppl. material 2.

## Grouping of MS<sup>2</sup> scans

In order to group MS<sup>2</sup> scans that presumably derive from the same substance, MS<sup>2</sup> scans with precursor ion  $m/z$  within 15 ppm and within 1.5% deviation in retention times were added together, and afterwards manually checked. In these grouped MS<sup>2</sup> scans, fragment ions that were within 15 ppm  $m/z$  were considered identical, their intensities added, and their masses recalculated by weighted mean averaging:

$$(m/z)_{avg} = \frac{\sum_{i=1}^N int_i \times (m/z)_i}{N}$$

where  $(m/z)_{avg}$  is the recalculated  $m/z$  value,  $(m/z)_i$  and  $int_i$  are the  $m/z$  and the intensity of the  $i^{\text{th}}$  fragment ion, respectively. Fragment ions having an intensity < 0.5% and a mass < 90 Da were excluded. The retention time of

the precursor ion with the highest intensity was chosen as the retention time of the grouped MS<sup>2</sup> scans.

## Used abbreviations

For simplicity and clarity of the presentation, the following abbreviations are used throughout this paper: hydroxycinnamic acid: HCA; coumaroyl: C; caffeoyl: A; glucosyl: G; feruloyl: F; 5,6-dihydroxyindole: I.

## Results and discussion

A workflow diagram of the study is shown in Fig. 1. In summary, hydromethanolic extract of purslane were obtained, and subjected to HR-MS<sup>2</sup> analysis, in both negative and positive ionization modes. After file transformation of the raw MS<sup>2</sup> data, DIF and DDF were applied. This was achieved either with MS<sup>2</sup>Analyzer, MZmine or an in-house Script in R programming language (details of the used script, together with example data are detailed in the Suppl. material 2). The filtered MS<sup>2</sup> data were then grouped based on a ppm and retention time threshold and analyzed manually to tentatively identify compounds that belong to the oleraindole class.

Oleraindoles are characterized by 5,6-dihydroxyindole, and similarly to oleraceins are *N*-acetylated with either coumaric, caffeic, or ferulic acid (Scheme 1). In refining the MS<sup>2</sup> raw data for compounds bearing oleraindole structure, DIF was applied based on the specific fragment ion for 5,6-dihydroxyindole: 148.04040  $m/z$  ( $C_8H_6NO_2^-$ ) for negative ionization mode, and 150.05495  $m/z$  ( $C_8H_8NO_2^+$ ) for positive ionization mode (Fig. 2). The error threshold was set to  $\pm 15$  ppm. Afterwards, the data was filtered based on the occurrence of a specific diagnostic difference (DDF) set to 149.04768 Da that suggested a neutral loss of 5,6-dihydroxyindole in the fragmentation process (Fig. 2). DDF was based on the detection of the specified  $m/z$  difference between each fragment (including the precursor ion, even if it was not present in the MS<sup>2</sup> spectrum) and all lower  $m/z$  fragment ions. DDF was achieved either with MS<sup>2</sup> Analyzer, or with a home-made script in the R programming language. The defined threshold was

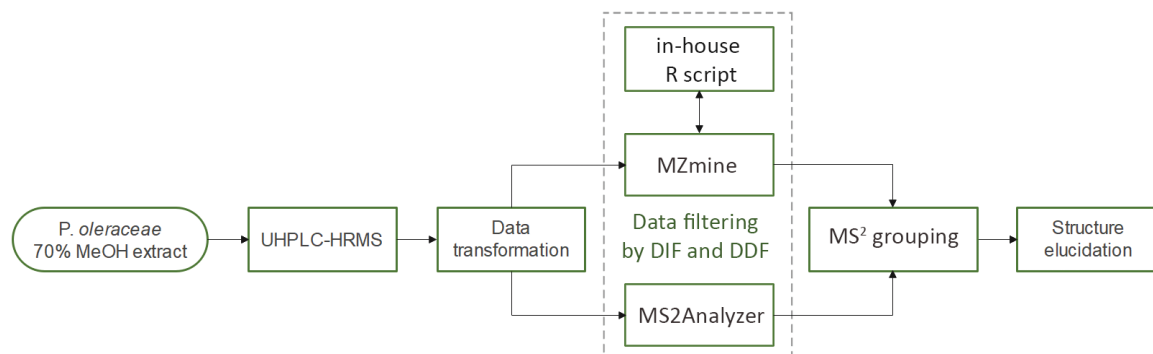


**Figure 1.** Workflow chart of the study. The hydromethanolic extract of purslane was subjected to UHPLC-HRMS with subsequent MS<sup>2</sup> analysis. After the raw data files were transformed with MSconvert, the data filtering (DIF and DDF) were performed either with MS<sup>2</sup>Analyzer, MZmine and the in-house R script. The scans that fell within 1.5% retention time threshold and 15 ppm  $m/z$  threshold were grouped, as belonging to the same substance. Then, the obtained list of possible oleraindole structures were manually inspected with the Xcalibur software.

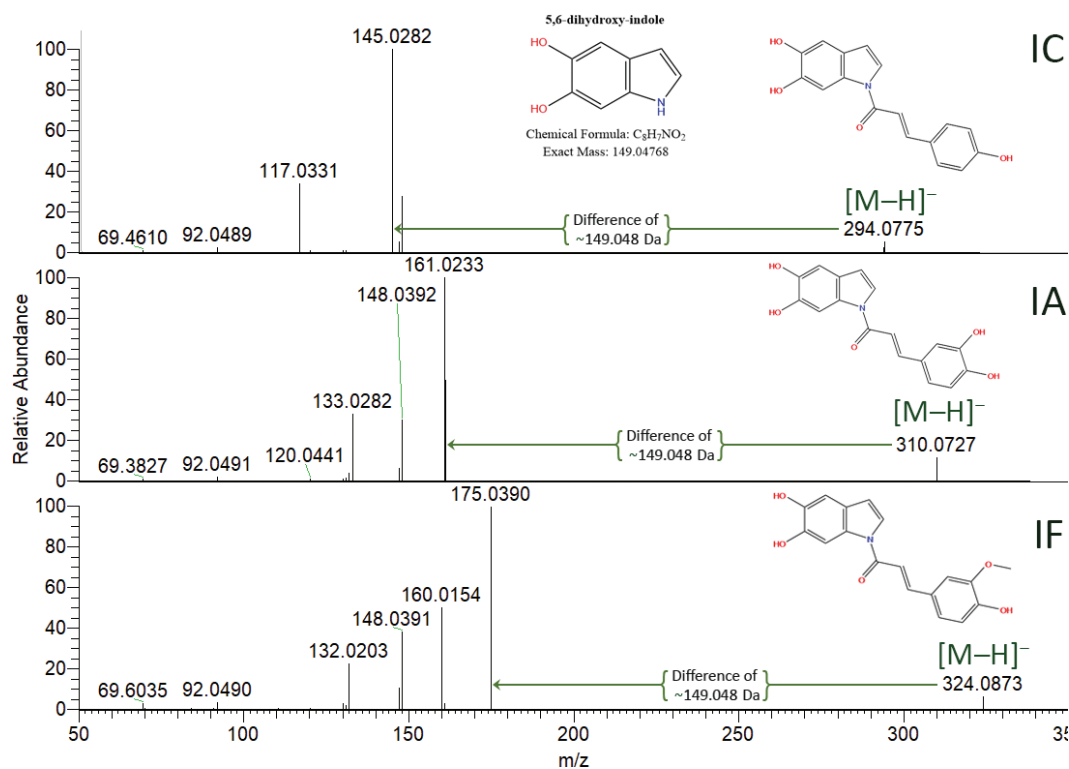


**Figure 2.** MS<sup>2</sup> spectra and fragmentation analysis of the three basic HCA-I conjugates in negative ionization mode. The characteristic difference of 149.048 Da, indicating a neutral loss of the 5,6-dihydroxyindole is indicated. The fragment ion corresponding to 5,6-dihydroxyindole is 148.04 m/z.

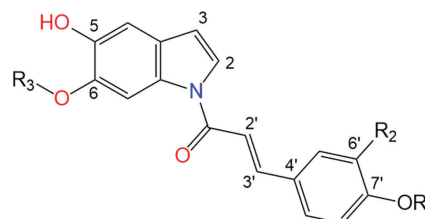
set to  $\pm 15$  ppm of the ions from which the difference originated. For example, in the fragmentation transition of 294.077 ([IC-H]<sup>-</sup>)  $\rightarrow$  145.028 ([C-H]<sup>-</sup>) *m/z* (Table 2), with a threshold of  $\pm 15$  ppm, the searched difference was between  $145.028 \pm 15$  ppm and  $294.077 \pm 15$  ppm (i.e., from 149.043 Da to 149.055 Da), whereas in the fragmentation transition of 324.093 ([IC-H]<sup>-</sup>)  $\rightarrow$  175.036 ([C-H]<sup>-</sup>) *m/z*, with a threshold of  $\pm 15$  ppm, the searched difference would be between  $175.036 \pm 15$  ppm and  $324.093 \pm 15$  ppm (i.e., from 149.041 Da to 149.057 Da). And so, if the difference originated from heavier fragment ions, a bigger mass (Da) threshold was used, and *vice versa*.

MS<sup>2</sup> spectra of I-HCA conjugates (IC, IA, and IF). The *m/z* difference search was set to  $149.04768 \pm 15$  ppm of the ions from which the difference originated. For IC: 149.0556 to 149.0424 Da; for IA: 149.0561 to 149.0419 Da; for IF: 149.0565 to 149.0415 Da.

Like oleraceins, all detected oleraindoles had the 5,6-dihydroxyindole *N*-acetylated with either coumaric, caffeic or ferulic acid. The sugar moieties are presumed to be glucoses, as in all isolated glucosylated oleraceins (Xiang et al. 2005; Jiao et al. 2015; Fu et al. 2021), and as characterized in oleraindole D (Xu et al. 2020b). After an in-depth MS<sup>2</sup> analysis, a total of 8 oleraindole compounds were tentatively identified and characterized. Our study limited the characterization of oleraindoles with mass up to 1kDa. Since oleraindole A is the lowest molecular weight representative with a monoisotopic mass of 295.08446 Da, the Full-scan mass detection range was set to 290–1000 *m/z*.

In total of 16 candidate substances were automatically selected, based on the above-mentioned criteria using

DIE, followed by DDF, and their MS<sup>2</sup> fragmentation manually inspected. Of the total 16 candidates, 3 had too low MS<sup>2</sup> intensity (below 1.5E04) and were not interpreted, 5 were false positives, and 8 were identified as oleraindoles (see Table 2 and Suppl. material 1). Of them, 2 structures are undescribed in the literature (GIA, and FGGIC), and the other 6 structures (IC, IA, IF, GIF, GIC, GIA and GGIC) match the structures of previously characterized oleraindoles. Table 1 presents the chemical structures of the identified 8 oleraindoles and Table 2 provides their chromatographic and mass spectral characteristics.



**Scheme 1.** Common scaffold of an oleraindole.

**Table 1.** List of the tentatively identified 8 oleraindoles, four of which are undescribed in the literature structures.

| Compound | R <sub>1</sub> | R <sub>2</sub>   | R <sub>3</sub> | Structure match                                 |
|----------|----------------|------------------|----------------|---|
| 1 IC     | H              | H                | H              | Oleraindole A (Zhao et al. 2019)                |
| 2 IA     | H              | OH               | H              | Oleraindole C (Xu et al. 2020a)                 |
| 3 IF     | H              | OCH <sub>3</sub> | H              | Oleraindole B (Zhao et al. 2019)                |
| 4 GIC    | H              | H                | glu            | (Lan et al. 2022b)                              |
| 5 GIA    | H              | OH               | glu            | this paper                                      |
| 6 GIF    | H              | OCH <sub>3</sub> | glu            | Oleraindole D (Xu et al. 2020b)                 |
| 7 GGIC   | H              | H                | glu-glu        | $\beta$ -D-Glc-Oleraindole G (Lan et al. 2022a) |
| 8 FGGIC  | H              | H                | fer-glu-glu    | this paper                                      |

**Table 2.** Mass spectral and chromatographic characteristics of the tentatively identified 9 oleraindoles. The transitions, corresponding to the neutral loss (-149.083 Da) of the 5,6-dihydroxyindole, are also provided.

| Abbrev. (elem. comp.) | Polarity | Molecular ion | Exact mass | ppm   | MS <sup>2</sup>  | Rt (min) | Transitions       |
|-----------------------|----------|---------------|------------|-------|--|----------|-------------------|
| IF (C18H15NO5)        | pos      | 326.1031      | 326.1023   | 2.45  | 326.1023 (5.45), 177.0546 (100), 150.0550 (2.11), 149.0597 (4.43), 145.0284 (20.74), 117.0335 (21.26), 91.0542 (0.91)                                  | 20.25    | 326.102 → 177.055 |
|                       | neg      | 324.0883      | 324.0877   | 1.85  | 324.0878 (5.87), 175.0391 (100), 161.0234 (2.47), 160.0156 (22.57), 148.0392 (25.84), 147.0314 (6.67), 132.0204 (15.23), 92.0490 (1.91)                | 20.25    | 324.088 → 175.039 |
| IC (C17H13NO4)        | pos      | 296.0925      | 296.0918   | 2.36  | 296.0917 (3.81), 150.0550 (2.65), 147.0441 (100), 119.0491 (22.15), 91.0542 (19.87)  | 19.41    | 296.092 → 147.044 |
|                       | neg      | 294.0781      | 294.0772   | 3.06  | 294.0774 (4.98), 148.0392 (20.4), 147.0314 (5.45), 145.0283 (100), 117.0331 (25.11), 92.0490 (1.88)  | 19.37    | 294.077 → 145.028 |
| IA (C17H13NO5)        | pos      | 312.0880      | 312.0867   | 4.17  | 312.0867 (6.77), 177.0546 (7.52), 163.0390 (100), 150.0550 (18.04), 145.0284 (6.62), 135.0441 (14.55), 117.0335 (11.86), 107.0491 (1.58)               | 16.48    | 312.087 → 163.039 |
|                       | neg      | 310.0729      | 310.0721   | 2.58  | 310.0724 (10.42), 161.0234 (100), 148.0392 (24.62), 147.0314 (5.09), 133.0282 (23.76), 132.0204 (2.77), 92.0490 (2.27)                                 | 16.5     | 310.072 → 161.023 |
| GIF (C24H25NO10)      | pos      | 488.1570      | 488.1552   | 3.69  | 326.1023 (9.48), 177.0546 (100), 150.0550 (1.93), 149.0597 (5), 145.0284 (18.94), 135.0441 (1.3), 117.0335 (20.58)                                     | 13.61    | 326.102 → 177.056 |
|                       | neg      | 486.1413      | 486.1406   | 1.44  | 324.0878 (95.67), 175.0391 (100), 161.0234 (8.83), 160.0156 (38.8), 148.0392 (18.07), 147.0314 (7.4), 133.0282 (2.2), 132.0204 (21.02), 92.0490 (1.65) | 13.62    | 324.088 → 175.039 |
| GIC (C23H23NO9)       | pos      | 458.1453      | 458.1446   | 1.53  | 296.0917 (10.52), 150.0550 (1.88), 147.0441 (100), 119.0491 (22.74), 91.0542 (13.6)  | 12.91    | 296.092 → 147.044 |
|                       | neg      | 456.1307      | 456.13     | 1.53  | 294.0774 (80.95), 148.0392 (13.75), 147.0314 (5.25), 145.0283 (100), 117.0331 (29.38)  | 12.89    | 294.077 → 145.028 |
| GIA (C23H23NO10)      | neg      | 472.124       | 472.1249   | -1.91 | 310.0724 (100), 161.0234 (92.53), 148.0392 (37.56), 133.0282 (27.9)  | 13.85    | 310.072 → 161.023 |
| GGIC (C29H33NO14)     | neg      | 618.1828      | 618.1828   | 0     | 294.0774 (65.77), 148.0392 (33.25), 145.0283 (100), 117.0331 (43.68)   | 14.16    | 294.077 → 145.028 |
| FGGIC (C39H41NO17)    | neg      | 794.2279      | 794.2302   | -2.9  | 618.1824 (2.09), 294.0774 (42.06), 175.0391 (17.35), 160.0154 (2.93), 148.0391 (18.67), 145.0282 (100), 117.0330 (3.6)                                 | 16.5     | 294.077 → 145.028 |

## Diagnostic fragment ions and transitions

After an in-depth MS<sup>2</sup> analysis and tentative characterization of oleraindole compounds, diagnostic fragment ions were selected, their elemental composition, and hence, their exact mass determined (Fig. 3 and Table 3). Table 2 presents the chromatographic and mass spectral data for the tentatively identified 8 oleraindoles with the exact masses of the diagnostic ions. In Suppl. material 1 are given the raw MS<sup>2</sup> spectra in positive and negative ionization mode.

Herein, the diagnostic fragment ions for the corresponding substructures are described. For negative ionization mode, the coumaroyl (C) moiety at 145.0295 m/z can cleave a CO to result in fragment ion 117.0346 m/z. The caffeoyl (A) is evident from fragment 161.0244 m/z, that can lose a CO (-27.9949 Da), to result in 133.0295 m/z. The latter can repulse a hydrogen radical to result in fragment 132.0217 m/z. The feruloyl (F) moiety is evident from fragment 175.0401 m/z, which can lose a CH<sub>2</sub>, or a methyl radical, to result in fragment ions 161.0244, or 160.0166 m/z, respectively. Fragment ion 161.0244 m/z can follow the fragmentation described above for A, and fragment ion 160.0166 can cleave a CO to result in 132.0217 m/z. The 5,6-dihydroxyindole substructure is represented with fragment 148.0404 m/z. The latter can repulse a hydrogen radical, or cleave a CO, to result in fragment ions 147.0326, or 92.0506 m/z, respectively.

For positive ionization mode, the coumaroyl (C) moiety at 147.0441 m/z can endure two consecutive CO losses

in the transition 147.0441 → 119.0491 → 91.0542 m/z. The caffeoyl (A) is evident from fragment ion 163.0390 m/z that can sustain a permutation of two CO and one water losses, resulting in the series of transitions outlined in Fig. 3. In a similar fashion, the feruloyl (F) moiety at 175.0401 m/z, can lose a CH<sub>3</sub>OH and CO, resulting in the transition 177.0546 → (145.0284 or 149.0597) → 117.0335 m/z, respectively. The latter is able to cleave CO, resulting in 89.0386 m/z. The 5,6-dihydroxyindole substructure is represented with fragment ion 150.0550 m/z.

## Individual MS<sup>2</sup> fragmentation analysis

Here, the individual MS<sup>2</sup> fragmentation analyses of the 8 tentatively identified by UHPLC-Orbitrap-MS oleraindoles are presented in increasing mass. For the HCA-I structures (IC, IA, and IF), the MS<sup>2</sup> elucidation follows the diagnostic ions as described above. In the elucidation of the glucosylated HCA-I structures (GIC, GIA, and GIF), the fragmentation is identical to their corresponding HCA-I, where a m/z difference of 162.053 Da, corresponding to the cleavage of a G moiety, is observed between the molecular ion and the HCA-I (i.e., GIC → IC). Compounds GGIC and FGGIC were evident in negative, but not in positive ionization mode. The fragmentation behavior of GGIC proceeds through a cleavage of the proximal GG (-324.107 Da) from the molecular ion at 618.1828 [M-H]<sup>-</sup> m/z to result in fragment ion 294.0774 m/z (IC). The following fragmentation of IC proceeds as described above. In the FGGIC structure, initially, there is a F cleavage from the molecular ion at

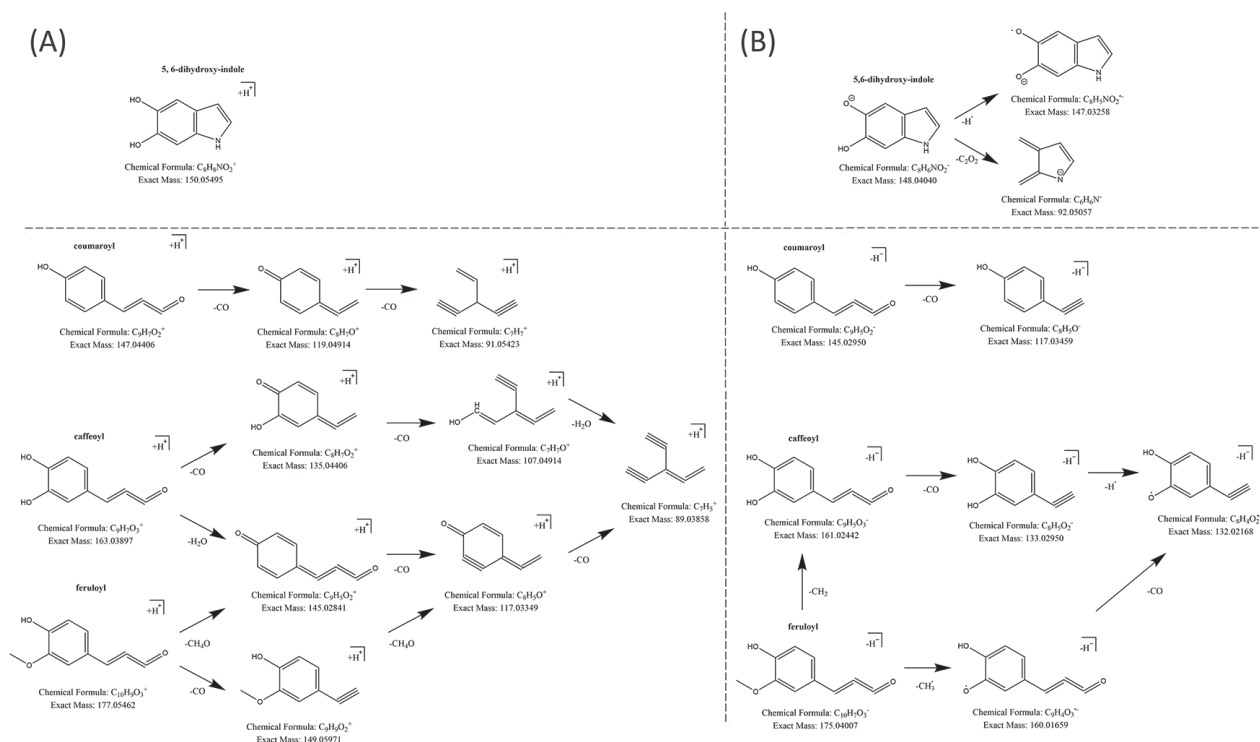


**Figure 3.** Proposed fragmentation behavior and diagnostic fragment ions of the basic components of oleraindoles: 5,6-dihydroxy-indole, and coumaroyl, caffeoyl, and feruloyl moieties. (A): negative ionization mode; (B): positive ionization mode.

**Table 3.** Exact mass and elemental composition of diagnostic fragment ions corresponding to oleraindole substructures.

| Substr. | Neg  | Pos  |
|---------|--|--|
| I       | 148.0404 (C <sub>8</sub> H <sub>6</sub> NO <sub>2</sub> <sup>-</sup> ), 147.0326 (C <sub>8</sub> H <sub>5</sub> NO <sub>2</sub> <sup>•-</sup> ), 92.0506 (C <sub>6</sub> H <sub>6</sub> N <sup>-</sup> )   | 150.055 (C <sub>8</sub> H <sub>8</sub> NO <sub>2</sub> <sup>+</sup> )  |
| C       | 145.0295 (C <sub>9</sub> H <sub>5</sub> O <sub>2</sub> <sup>-</sup> ), 117.0346 (C <sub>8</sub> H <sub>5</sub> O <sup>-</sup> )  | 147.0441 (C <sub>9</sub> H <sub>7</sub> O <sub>2</sub> <sup>+</sup> ), 119.0491 (C <sub>8</sub> H <sub>7</sub> O <sup>+</sup> ), 91.0542 (C <sub>7</sub> H <sub>7</sub> <sup>+</sup> )   |
| A       | 161.0244 (C <sub>9</sub> H <sub>5</sub> O <sub>3</sub> <sup>-</sup> ), 133.0295 (C <sub>8</sub> H <sub>5</sub> O <sub>2</sub> <sup>-</sup> ), 132.0217 (C <sub>8</sub> H <sub>4</sub> O <sub>2</sub> <sup>•-</sup> )   | 163.039 (C <sub>9</sub> H <sub>7</sub> O <sub>3</sub> <sup>+</sup> ), 145.0284 (C <sub>9</sub> H <sub>5</sub> O <sub>2</sub> <sup>+</sup> ), 135.0441 (C <sub>8</sub> H <sub>7</sub> O <sub>2</sub> <sup>+</sup> ), 117.0335 (C <sub>8</sub> H <sub>5</sub> O <sup>+</sup> ), 107.0491 (C <sub>7</sub> H <sub>7</sub> O <sup>+</sup> ), 89.0386 (C <sub>7</sub> H <sub>5</sub> <sup>+</sup> )  |
| F       | 175.0401 (C <sub>10</sub> H <sub>7</sub> O <sub>3</sub> <sup>-</sup> ), 161.0244 (C <sub>9</sub> H <sub>5</sub> O <sub>3</sub> <sup>-</sup> ), 160.0166 (C <sub>9</sub> H <sub>4</sub> O <sub>3</sub> <sup>•-</sup> ), 133.0295 (C <sub>8</sub> H <sub>5</sub> O <sub>2</sub> <sup>-</sup> ), 132.0217 (C <sub>8</sub> H <sub>4</sub> O <sub>2</sub> <sup>•-</sup> ) | 177.0546 (C <sub>10</sub> H <sub>9</sub> O <sub>3</sub> <sup>+</sup> ), 149.0597 (C <sub>9</sub> H <sub>9</sub> O <sub>2</sub> <sup>+</sup> ), 145.0284 (C <sub>9</sub> H <sub>5</sub> O <sub>2</sub> <sup>+</sup> ), 135.0441 (C <sub>8</sub> H <sub>7</sub> O <sub>2</sub> <sup>+</sup> ), 117.0335 (C <sub>8</sub> H <sub>5</sub> O <sup>+</sup> ), 107.0491 (C <sub>7</sub> H <sub>7</sub> O <sup>+</sup> ), 89.0386 (C <sub>7</sub> H <sub>5</sub> <sup>+</sup> ) |
| IC      | 294.0771 (C <sub>17</sub> H <sub>12</sub> NO <sub>4</sub> <sup>-</sup> )   | 296.0917 (C <sub>17</sub> H <sub>14</sub> NO <sub>4</sub> <sup>+</sup> )   |
| IA      | 310.072 (C <sub>17</sub> H <sub>12</sub> NO <sub>5</sub> <sup>-</sup> )  | 312.0867 (C <sub>17</sub> H <sub>14</sub> NO <sub>5</sub> <sup>+</sup> )   |
| IF      | 324.0877 (C <sub>18</sub> H <sub>14</sub> NO <sub>5</sub> <sup>-</sup> )   | 326.1023 (C <sub>18</sub> H <sub>16</sub> NO <sub>5</sub> <sup>+</sup> )   |

794.2302 [M-H]<sup>-</sup> m/z, to result in fragment ion 618.1828 m/z (GGIC). The fragmentation of the latter continues as described above.

## Conclusion

Herein, utilizing UHPLC-Orbitrap-HRMS technique, in both negative and positive ionization modes, eight oleraindole compounds were tentatively identified in hydro-methanolic extracts of purslane, of which 2 structures are

described for the first time. Diagnostic ion filtering (DIF) and diagnostic difference filtering (DDF) were utilized to filter out MS data, using data analysis tools.

## Acknowledgement

This work was financed by the European Union NextGenerationEU through the National Recovery and Resilience Plan of the Republic of Bulgaria, project No. BG-RRP-2.004-0004-C01.

## References

- Akbar S (2020) *Portulaca oleracea* L. (Portulacaceae). Handbook of 200 Medicinal Plants: A Comprehensive Review of Their Traditional Medical Uses and Scientific Justifications. Springer International Publishing, Cham, 1491–1504. [https://doi.org/10.1007/978-3-030-16807-0\\_154](https://doi.org/10.1007/978-3-030-16807-0_154)
- Corrado G, El-Nakhel C, Graziani G, Pannico A, Zarrelli A, Giannini P, Ritieni A, De Pascale S, Kyriacou MC, Roupheal Y (2021) Productive and morphometric traits, mineral composition and secondary

metabolome components of borage and purslane as underutilized species for microgreens production. Horticulturae 7: e211. <https://doi.org/10.3390/horticulturae7080211>

- Farag MA, Shakour ZTA (2019) Metabolomics driven analysis of 11 *Portulaca* leaf taxa as analysed via UPLC-ESI-MS/MS and chemometrics. Phytochemistry 161: 117–129. <https://doi.org/10.1016/j.phytochem.2019.02.009>

- French WR, Zimmerman LJ, Schilling B, Gibson BW, Miller CA, Townsend RR, Sherrod SD, Goodwin CR, McLean JA, Tabb DL (2015) Wavelet-based peak detection and a new charge inference procedure for MS/MS implemented in ProteoWizard's msConvert. *Journal of proteome research* 14: 1299–1307. <https://doi.org/10.1021/pr500886y>
- Fu J, Wang H, Dong C, Xi C, Xie J, Lai S, Chen R, Kang J (2021) Water-soluble alkaloids isolated from *Portulaca oleracea* L. *Bioorganic Chemistry* 113: e105023. <https://doi.org/10.1016/j.bioorg.2021.105023>
- Jiao Z-Z, Yue S, Sun H-X, Jin T-Y, Wang H-N, Zhu R-X, Xiang L (2015) Indoline amide glucosides from *Portulaca oleracea*: Isolation, structure, and DPPH Radical scavenging activity. *Journal of Natural Products* 78: 2588–2597. <https://doi.org/10.1021/acs.jnatprod.5b00524>
- Jiao Z, Wang H, Wang P, Sun H, Yue S, Xiang L (2014) Detection and quantification of cyclo-dopa amides in *Portulaca oleracea* L. by HPLC-DAD and HPLC-ESI-MS/MS. *J 中国药学*: 3. <https://doi.org/10.5246/jcps.2014.08.069>
- Kumar A, Sreedharan S, Kashyap AK, Singh P, Ramchiary N (2021) A review on bioactive phytochemicals, ethnomedicinal and pharmacological importance of Purslane (*Portulaca oleracea* L.). [Preprint (Version 1)] <https://doi.org/10.21203/rs.3.rs-501982/v1>
- Lan X, Guo S, Song M, Liu P, Tian J, Zhang W, Ying X (2022a) A novel amide alkaloid from *Portulaca oleracea*. *Chemistry of Natural Compounds* 58: 1089–1092. <https://doi.org/10.1007/s10600-022-03873-w>
- Lan X, Ying Z, Guo S, Duan Y, Cui X, Leng A, Ying X (2022b) Two novel amide alkaloids from *Portulaca oleracea* L. and their anti-inflammatory activities. *Natural product research* 36: 5567–5574. <https://doi.org/10.1080/14786419.2021.2021519>
- Ma Y, Kind T, Yang D, Leon C, Fiehn OJAc (2014) MS2Analyzer: A software for small molecule substructure annotations from accurate tandem mass spectra *ACS Publications* 86: 10724–10731. <https://doi.org/10.1021/ac502818e>
- Melilli MG, Di Stefano V, Sciacca F, Pagliaro A, Bognanni R, Scandurra S, Virzì N, Gentile C, Palumbo M (2020) Improvement of fatty acid profile in durum wheat breads supplemented with *Portulaca oleracea* L. quality traits of purslane-fortified bread. *Foods* 9: e764. <https://doi.org/10.3390/foods9060764>
- Perez de Souza L, Naake T, Tohge T, Fernie ARJG (2017) From chromatogram to analyte to metabolite. How to pick horses for courses from the massive web resources for mass spectral plant metabolomics. *GigaScience* 6: gix037. <https://doi.org/10.1093/gigascience/gix037>
- Petropoulos SA, Fernandes Â, Dias MI, Vasilakoglou IB, Petrotos K, Barros L, Ferreira IC (2019) Nutritional value, chemical composition and cytotoxic properties of common purslane (*Portulaca oleracea* L.) in relation to harvesting stage and plant part. *Antioxidants* 8: e293. <https://doi.org/10.3390/antiox8080293>
- Pluskal T, Castillo S, Villar-Briones A, Oresic M (2010) MZmine 2: modular framework for processing, visualizing, and analyzing mass spectrometry-based molecular profile data. *BMC Bioinformatics* 11: e395. <https://doi.org/10.1186/1471-2105-11-395>
- Stein S (2012) Mass Spectral Reference Libraries: An Ever-Expanding Resource for Chemical Identification. *Analytical Chemistry* 84: 7274–7282. <https://doi.org/10.1021/ac301205z>
- Voynikov Y, Gevrenova R, Balabanova V, Doytchinova I, Nedialkov P, Zheleva-Dimitrova D (2019) LC-MS analysis of phenolic compounds and oleraceins in aerial parts of *Portulaca oleracea* L. *Journal of Applied Botany Food Quality* 92: 298–312.
- Voynikov Y, Nedialkov P, Gevrenova R, Zheleva-Dimitrova D, Balabanova V, Dimitrov I (2021a) UHPLC-Orbitrap-HRMS Identification of 51 Oleraceins (Cyclo-Dopa Amides) in *Portulaca oleracea* L. Cluster Analysis and MS2 Filtering by Mass Difference 10: e1921. <https://doi.org/10.20944/preprints202109.0048.v1>
- Voynikov Y, Nedialkov P, Gevrenova R, Zheleva-Dimitrova D, Balabanova V, Dimitrov I (2021b) UHPLC-Orbitrap-MS Tentative Identification of 51 Oleraceins (Cyclo-Dopa Amides) in *Portulaca oleracea* L. Cluster Analysis and MS2 Filtering by Mass Difference. *Plants* 10: e1921. <https://doi.org/10.3390/plants10091921>
- Xiang L, Xing D, Wang W, Wang R, Ding Y, Du L (2005) Alkaloids from *Portulaca oleracea* L. *Phytochemistry* 66: 2595–2601. <https://doi.org/10.1016/j.phytochem.2005.08.011>
- Xing J, Yang Z, Lv B, Xiang L (2008) Rapid screening for cyclo-dopa and diketopiperazine alkaloids in crude extracts of *Portulaca oleracea* L. using liquid chromatography/tandem mass spectrometry. *Rapid Communications in Mass Spectrometry* 22: 1415–1422. <https://doi.org/10.1002/rcm.3526>
- Xu W, Liu F, Wang H, Zhang W, He F, Ying X (2020a) A new indole alkaloid from *Portulaca oleracea* L. and its antiacetylcholinesterase activity. *Latin American Journal Of Pharmacy* 39: 591–595.
- Xu W, Ying Z, Tao X, Ying X, Yang G (2020b) Two new amide alkaloids from *Portulaca oleracea* L. and their anticholinesterase activities. *Natural Product Research* 35(21): 3794–3800. [1–7] <https://doi.org/10.1080/14786419.2020.1739040>
- Zhao C, Zhang C, He F, Zhang W, Leng A, Ying X (2019) Two new alkaloids from *Portulaca oleracea* L. and their bioactivities. *Fitoterapia* 136: e104166. <https://doi.org/10.1016/j.fitote.2019.05.005>

## Supplementary material 1

### MS/MS spectra of identified compounds

Authors: Yulian Voynikov, Reneta Gevrenova, Dimitrina Zheleva-Dimitrova, Vessela Balabanova, Irina Nikolova, Lyubomir Marinov, Iossif Benbassat, Georgi Momekov

Data type: docx

Copyright notice: This dataset is made available under the Open Database License (<http://opendatacommons.org/licenses/odbl/1.0>). The Open Database License (ODbL) is a license agreement intended to allow users to freely share, modify, and use this Dataset while maintaining this same freedom for others, provided that the original source and author(s) are credited.

Link: <https://doi.org/10.3897/pharmacia.70.e113577.suppl1>

## Supplementary material 2

### Scripts

Authors: Yulian Voynikov, Reneta Gevrenova, Dimitrina Zheleva-Dimitrova, Vessela Balabanova, Irina Nikolova, Lyubomir Marinov, Iossif Benbassat, Georgi Momekov

Data type: rar

Copyright notice: This dataset is made available under the Open Database License (<http://opendatacommons.org/licenses/odbl/1.0>). The Open Database License (ODbL) is a license agreement intended to allow users to freely share, modify, and use this Dataset while maintaining this same freedom for others, provided that the original source and author(s) are credited.

Link: <https://doi.org/10.3897/pharmacia.70.e113577.suppl2>